Supporting Information

Wormlike Porous and Defect-structured Cadmium Stannate Photoanodes for Enhanced Solar Water Oxidation

Pan Peng,[a,b,1] *Ping Wang,*[b,1,*] *Zhengyang Cai,*[a,b] *Jiajia Zhang,*[a] *Yu Hu,*[a] *Jingcheng Xu,*[a] *Xianying Wang*[b,*]

[a] School of Materials Science and Technology, University of Shanghai for Science and Technology, Jungong Rd. 516, 200093 Shanghai, P.R. China.

[b] Shanghai Institute of Ceramics, Chinese Academy of Sciences, Heshuo Rd. 585, 201899 Shanghai, P.R. China. Email: wangping@mail.sic.ac.cn; wangxianying@mail.sic.ac.cn

[1] These authors contributed equally.

Photoelectrochemical measurements

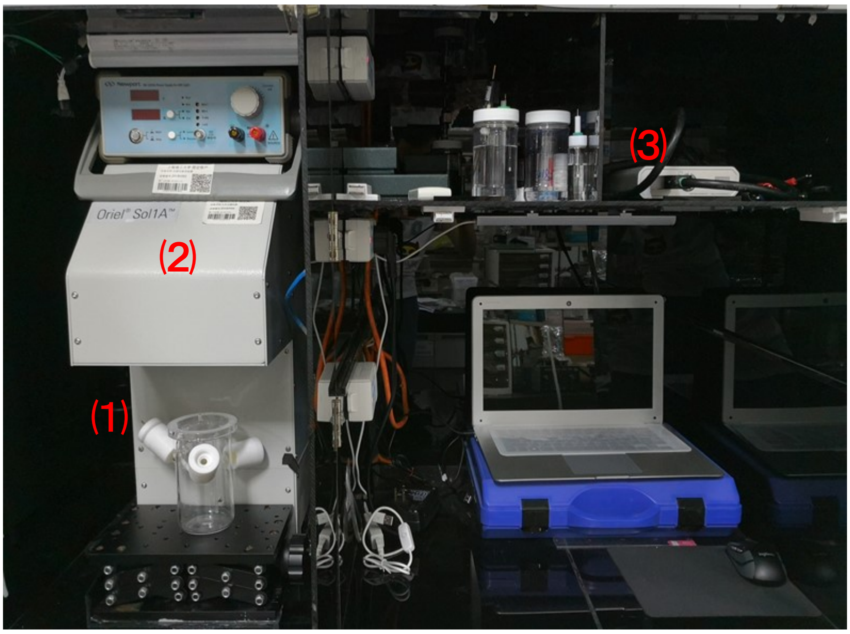

Measurement setup descriptions: (1) photocurrent-potential curves, electrochemical impedance spectra (EIS) and Mott-Schottky (MS) analysis were conducted in a standard three-electrode configuration system. (2) A Newport AM 1.5 G solar simulator (150 W Oriel model 94021A, Newport/Oriel instruments, USA) was used as a light source. (3) All the electrochemical tests were measured via a Ivium CompactStat potentiostat.

Electrochemical Impendence Spectra (EIS) analyses are carried out at 0 V vs SCE at afrequency range of 100 kHz to 0.1 Hz with an amplitude of 10 mV under AM 1.5G illumination.

Mott-Schottky measurements were carried out at a frequency of 1 kHz in dark. The donor densities were calculated by Mott-Schottky equation:

$$\frac{1}{C^2} = \frac{2}{e_0 \varepsilon \varepsilon_0 N_d}[(V - V_f) - \frac{kT}{e_0}]$$

$$N_d = \frac{2}{e_0 \varepsilon \varepsilon_0}[d\left(\frac{1}{C^2}\right)/dV]^{-1}$$

Where e_0 is the electron charge, $\varepsilon$is the relative permittivity of $BiVO_4$ (ε =68), ε_0 is the permittivity of vacuum, N_d is the donor density, V *is* the applied bias at the electrode, V_f is the flatband potential.

Charge efficiencies calculation

Bulk charge separation efficiency (η_{bulk}) and interfacial charge transfer efficiency $\eta_{surface}$ were calculated by the following equations:[1-2]

$$\eta_{bulk} = J_{ph}^{Na_2SO_3} / J_{abs}$$

$$\eta_{surface} = J_{ph}^{H_2O} / J_{ph}^{Na_2SO_3}$$

Where $J_{ph}^{H_2O}$ and $J_{ph}^{Na_2SO_3}$ are the photocurrent density measured in electrolyte solution without and with 0.1M Na_2SO_3 as a hole scavenger, respectively. J_{abs} is the photon absorption rate expressed as the photocurrent density, which was calculated by: $J_{abs} = \frac{q}{hc}\int_{\lambda} \lambda \cdot \phi_{\lambda} \cdot \eta_{abs} d\lambda$, where q is the charge of an electron, h is the Plank constant, c is the light speed, ϕ_{λ} is the photon flux of the AM 1.5G solar spectrum, η_{abs} is the absorbance of the photoanode.

Incident-photon-to-current-conversion efficiency

The incident-photon-to-current-conversion efficiency (IPCE) were performed by measuring the photocurrent density under monochromated light irradiation with a 500 W Xe arc lamp coupled into a grating monochromator, which were then calculated following the equation:

$$IPCE = \frac{1239.8(V \times nm) \times |j_{ph}(mA/cm^2)|}{\lambda(nm) \times P_{mono}(mW/cm^2)} \times 100\%$$

Where j_{ph} is the photocurrent density, λ the incident light wavelength, and P_{mono} is the calibrated and monochromated illumination power intensity[3]. The illumination intensities of the monochromatic light were measured with a PM 100A Optical Power Meter.

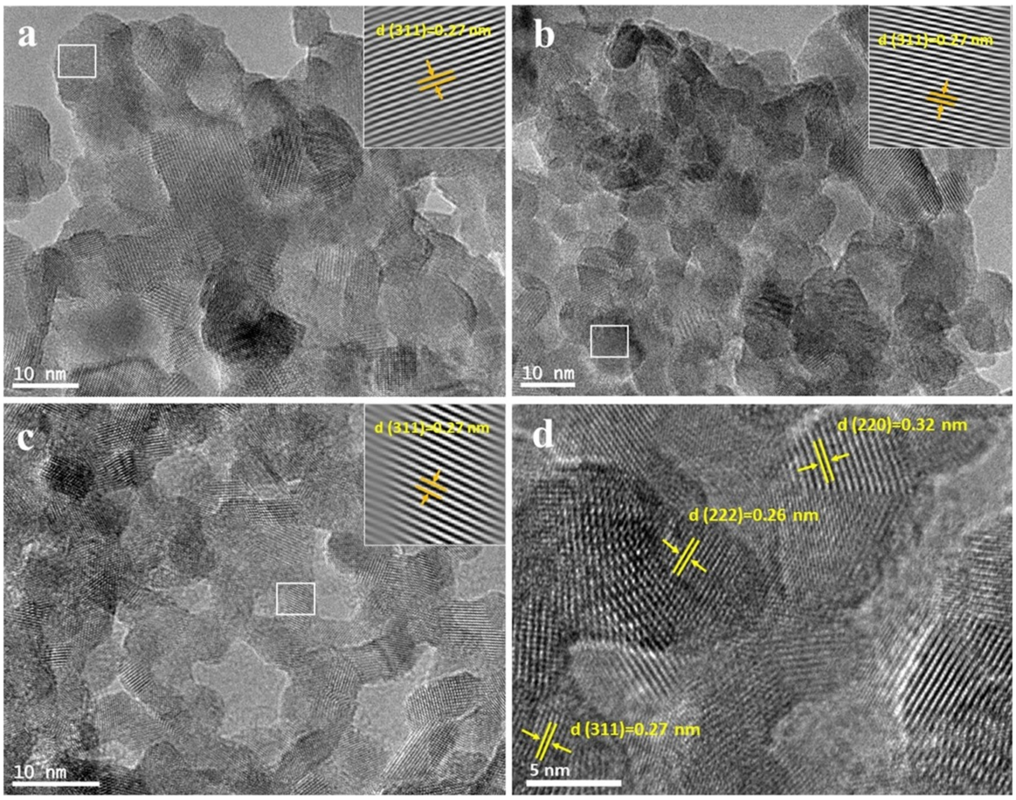

Figure S1. HRTEM image of (a) CTA500, (b) CTA500-HMA5, (c-d) HMA8 and the corresponding auto-correlated HRTEM lattice image (the inset).

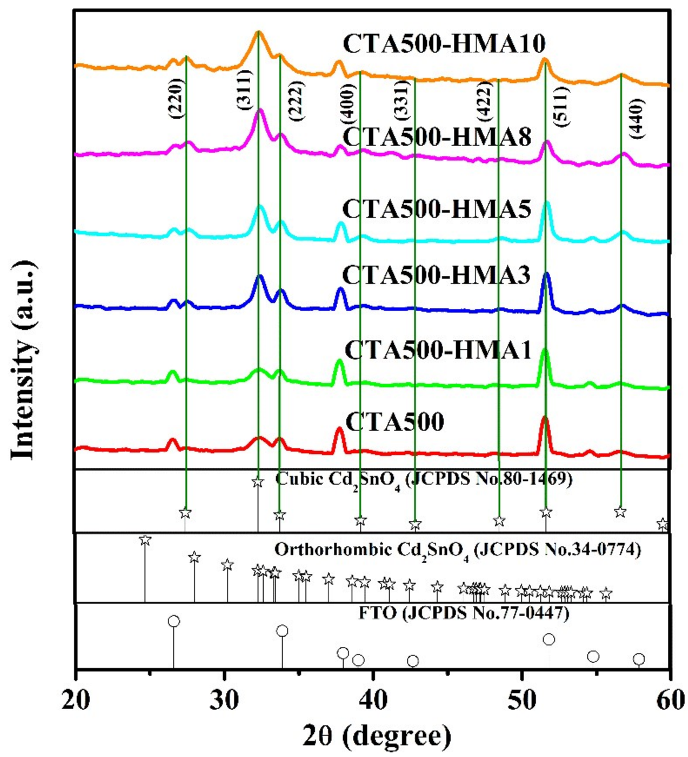

Figure S2. XRD patterns of CTA500, CTA500-HMA1, CTA500-HMA3, CTA500-HMA5, CTA500-HMA8, CTA500-HMA10 showing the formation of pure- phase cubic Cd_2SnO_4.

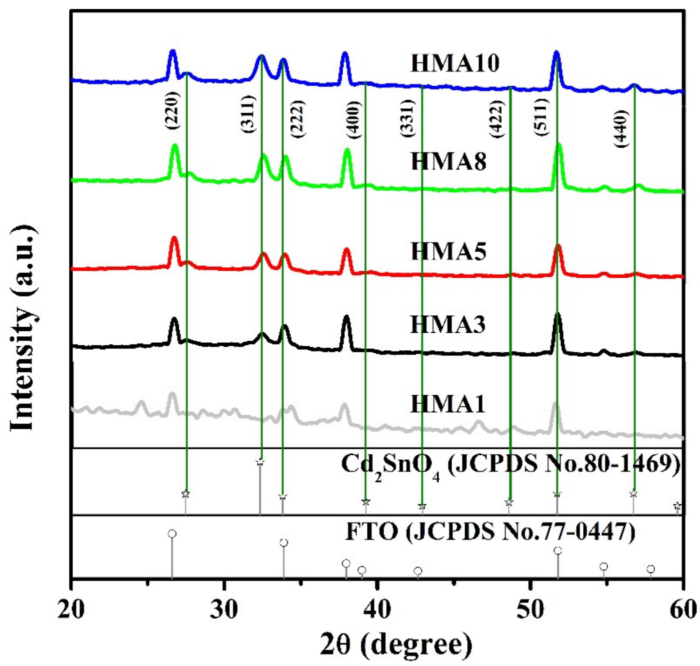

Figure S3. XRD patterns of HMAX samples with the prolonged HMA time, showing the formation of pure-phase cubic Cd_2SnO_4 in HMA3, HMA5, HMA8, and HMA10 samples, while large number of CdO impurities were co-existed in HMA1.

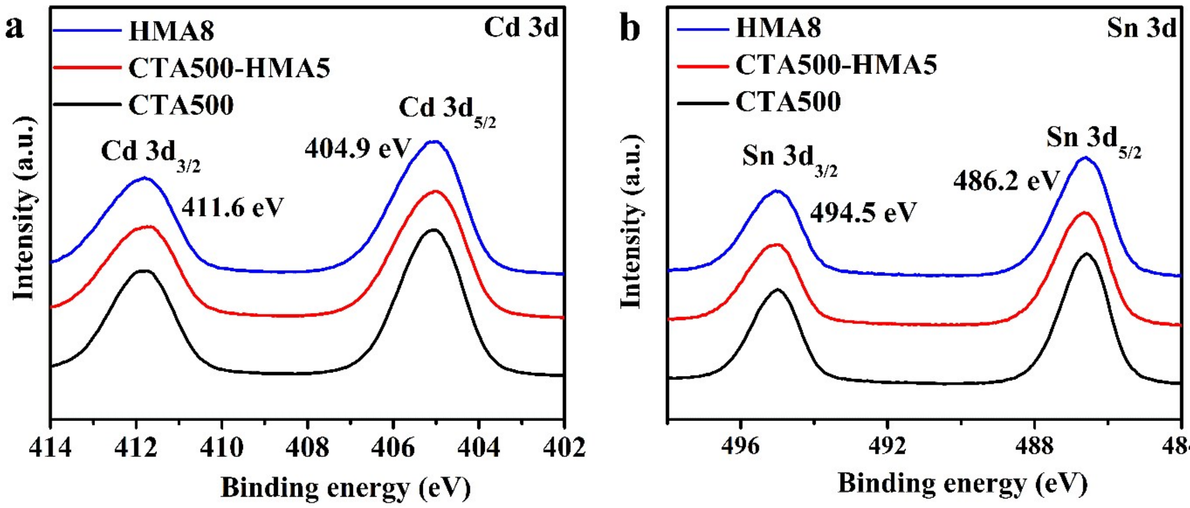

Figure S4. The narrow-scan XPS spectra of (a) Cd 3d and Sn 3d (b) in CTA500, CTA500-HMA5 and HMA8 samples.

Table S1. Atomic concentration (at%) of Cd and Sn elements derived from survey-scan XPS spectra.

At.%	**Cd**	**Sn**
CTA500	6.9	4.7
CTA500-HMA5	6.0	4.0
HMA8	7.0	4.7

Table S2. Atomic concentration (at%) of Cd and Sn elements obtained from ICP-OES.

At.%	**Cd**	**Sn**
CTA500	17.83	13.25
CTA500-HMA5	11.53	7.77
HMA8	14.32	10.26

Table S3. Atomic ratios of O_L, O_V and O_C calculated from the XPS spectra in Figure 2d.

Samples	O_L	O_v	O_c
CTA500	16.7	22.3	61.0
CTA500-HMA5	16.0	22.9	61.1
HMA8	14.4	24.4	61.2

Table S4. Estimation of conduction band (E_{CB}) and valence band (E_{VB}) of CTA500, CTA500-HMA5 and HMA8 samples by Mott-Schottky plots (MS) analysis.

Samples	E_{FB}(eV)	E_{CB}(eV)	E_{VB}(eV)
CTA500	-0.78	-0.88	1.72
CTA500-HMA5	-0.79	-0.89	1.65
HMA8	-0.80	-0.90	1.62

Table S5. Performance comparison with other typical photocatalytic materials.

Photoanodes ($C_{x=1,2,3}$)	Annealing method	J (μA cm^{-2})	$J_{x=1,2}$ (μA cm^{-2})	Ref.
Cd_2SnO_4(C_1/J_1)	**HMA (8min)**	**25**	**300**	**This Work**
	CTA (500°C, 2 h) & HMA (5 min)	**13**	**100**	
	CTA (500°C, 2 h)	**4**	**30**	
$BiVO_4$(C_2/J_1)	CTA (470°C, 5 h)	30	400	1
	HMA (6 min)	80	1400	
$ZnFe_2O_4$(C_3/J_2)	CTA (550°C, 3 h)	15	171	4
	CTA (800°C, 20 min)	25	50	

	CTA (550°C, 3 h) & HMA (5 min)	240	320	
Cd_2SnO_4 (J_3)	CTA (550°C, 2 h) & CTA (750°C, 2 h)		220	5
Cubic: Cd_2SnO_4 (C_4)	CTA (550°C, 2 h) & CTA (750°C, 2 h)	280		6
Ortho: Cd_2SnO_4 (C_4)	CTA (550°C, 2 h) & CTA (750°C,2 h) & CTA (1050°C, 2 h)	124		6
Cd_2SnO_4 (C_4)	CTA (550°C, 2 h) & CTA (750°C, 12 h)	357		6
$ZnFe_2O_4$(C_3)	HMA (2 min)	150		7
	CTA (850°C, 7.5 min)	40		
α-Fe_2O_3(C_3/J_2)	CTA (600°C, 1h)	13	60	8
	HMA (10 min)	320	580	

C_1:1 M KOH, 1.7 V_{RHE}; C_2:0.5 M KPi, 1.23 V_{RHE}; C_3:1 M KOH, 1.23 V_{RHE}; C_4:1 M NaOH, 0.6 V_{RHE}. J_1: Na_2SO_3 as the sacrificial reagent. J_2: H_2O_2 as a hole scavenger. J_3: 0.8 V_{RHE}, 0.24 M Na_2S and 0.35 M Na_2SO_3 electrolyte.

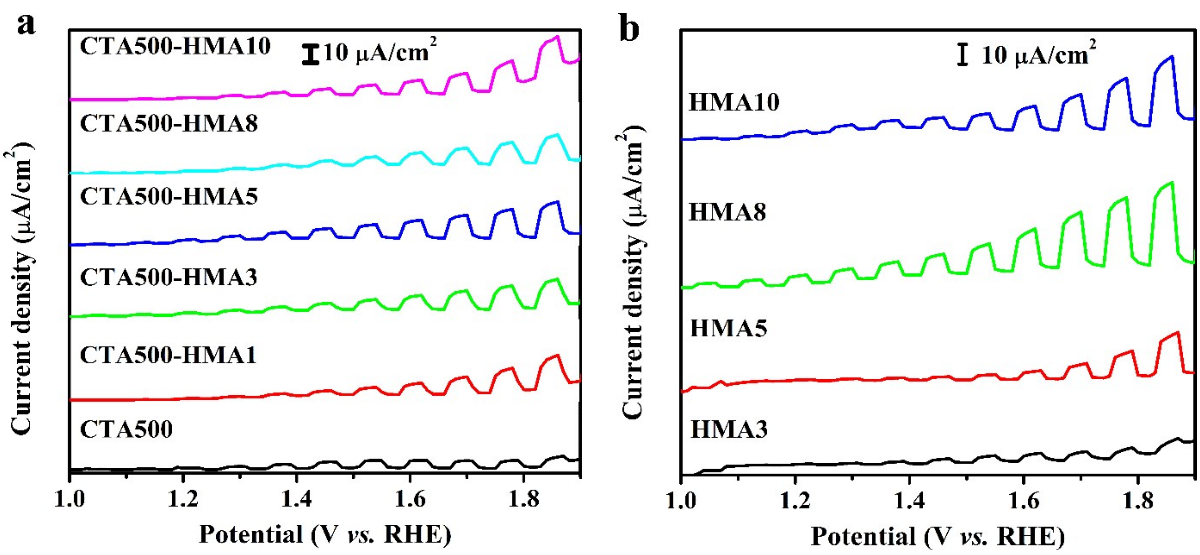

Figure S5. (a) Linear sweep voltammetry (LSV) curves of the Cd_2SnO_4 samples under chopped light illumination (1 sun) at the scanning rate of 10 mV/s. (b) LSV curves of HMA samples prepared at different HMA times under chopped light illumination (1 sun) at the scanning rate of 10 mV/s.

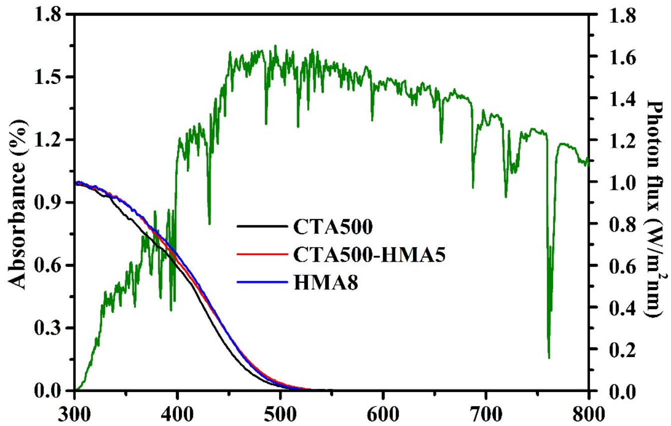

Figure S6. The J_{abs} values of CTA500, CTA500-HMA5 and HMA8 calculated to be 5.21, 5.61, and 5.63 mA/cm^2, respectively.

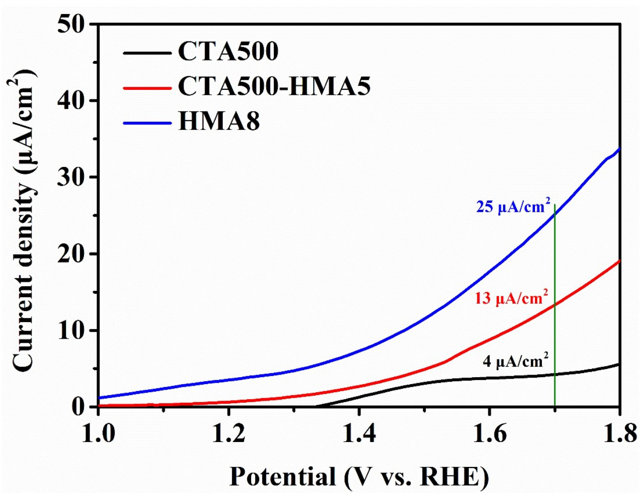

Figure S7. The LSV measurements of the recycled CTA500, CTA500-HMA5 and HMA8 after the stability test.

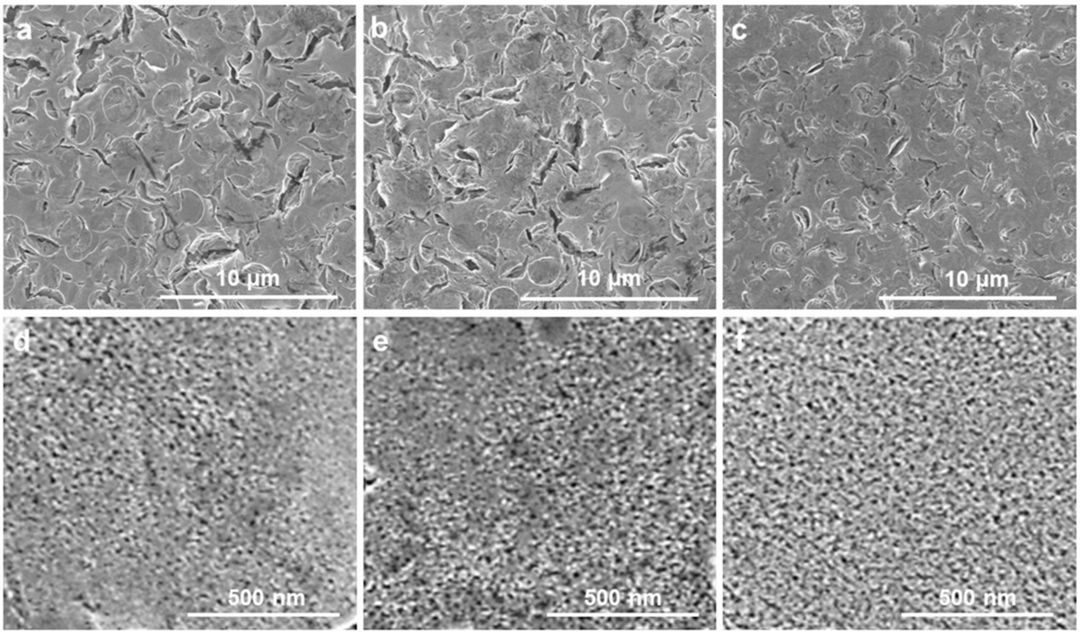

Figure S8. Typical SEM images of the recycled CTA500 (a, d), CTA500-HMA5 (b, e) and HMA8 (c, f).

REFERENCES

1. J. H. Kim, Y. H. Jo, J. H. Kim and J. S. Lee, *Nanoscale*, 2016, **8**, 17623-17631.
2. H. Zhang, H. Li, Z. Wang, Z. Zheng, P. Wang, Y. Liu, X. Zhang, X. Qin, Y. Dai and B. Huang, *Appl. Catal. B*, 2018, **238**, 586-591.
3. C. Jiang, S. J. Moniz, A. Wang, T. Zhang and J. Tang, *Chem. Soc. Rev.*, 2017, **46**, 4645-4660.
4. J. H. Kim, J. H. Kim, J. Jang, J. Y. Kim, S. H. Choi, G. Magesh, J. Lee, and J. S. Lee, *Adv. Energy Mater.*, 2015, **5**, 1401933.
5. S. Kelkar, C. Ballal, A. Deshpande, S. Warule and S. Ogale, *J. Mater. Chem. A*, 2013, **1**, 12426-124316.
6. A. Deshpande, S. Kelkar, S. Rayaluc and S. Ogale, *J. Mater. Chem. A*, 2014, **2**, 492-499.
7. J. H. Kim, Y. J. Jang, S. H. Choi, B. J. Lee, M. H. Lee, and J. S. Lee, *ACS Sustainable Chem. Eng.*, 2019, **7**, 944-949
8. K. Ramachandran, M. Geerthana, P. Maadeswaran, B. Liang and R. Ramesh, *Optik*, 2020, **212**, 164658.